γ-Al_2O_3-Supported Re−Pt Cluster Catalyst Prepared from $[Re_2Pt(CO)_{12}]$: Characterization by Extended X-ray Absorption Fine Structure Spectroscopy and Catalysis of Methylcyclohexane Dehydrogenation

A. S. Fung,[†] M. J. Kelley,[‡] D. C. Koningsberger,*[,§] and B. C. Gates*[,†,⊥]

Contribution from the Center for Catalytic Science and Technology, Department of Chemical Engineering, University of Delaware, Newark, Delaware 19716, E. I. du Pont de Nemours and Company, Wilmington, Delaware 19898, Debye Institute, Laboratory of Inorganic Chemistry and Catalysis, Utrecht University, P.O. Box 80083, 3508 TB Utrecht, The Netherlands, and Department of Chemical Engineering and Materials Science, University of California, Davis, California 95616

Received August 12, 1996[⊗]

Abstract: A model catalyst prepared from $[Re_2Pt(CO)_{12}]$ supported on γ-Al_2O_3 was characterized by extended X-ray absorption fine structure (EXAFS) spectroscopy, and its stability in operation in a flow reactor was tested for the dehydrogenation of methylcyclohexane at 1 atm and 400 °C. EXAFS data characterizing the unused catalyst measured at both the Re L_{III} and Pt L_{III} edges at liquid nitrogen temperature with the sample in the presence of H_2 distinguish the Re−Pt from the Pt−Pt and Re−Re interactions. The EXAFS results form the basis of a simplified model of the supported bimetallic structures, consisting of Re_4Pt_2 entities, with oxophilic Re in a low positive oxidation state interacting strongly with the oxygen atoms of the γ-Al_2O_3 support and stabilizing the dispersion of the Pt atoms. The catalyst made from $[Re_2Pt(CO)_{12}]$ was found to be more resistant to deactivation during catalytic dehydrogenation of methylcyclohexane than catalysts prepared conventionally from Re and Pt salt precursors. The catalyst prepared from $[Re_2Pt(CO)_{12}]$ was more highly dispersed than the others, and its resistance to deactivation is attributed to the role of Re in stabilizing the dispersion of the Pt.

Introduction

The addition of Re to Al_2O_3-supported Pt catalysts improves the activity maintenance in industrial naphtha reforming,[1] and Re−Pt/γ-Al_2O_3 is the predominant catalyst used for this process. However, notwithstanding years of research, the catalyst structure and the roles of Re remain elusive targets. In attempts to understand the role of Re better, we prepared model Re−Pt/γ-Al_2O_3 catalysts from $[Re_2Pt(CO)_{12}]$ and have already reported the synthesis and characterization by infrared spectroscopy, X-ray photoelectron spectroscopy, and temperature-programmed reduction together with the results for a comparable catalyst prepared from salt precursors.[2] These results demonstrate that $[Re_2Pt(CO)_{12}]$, following deposition on γ-Al_2O_3 and treatment in H_2 at 400 °C, was converted into small bimetallic entities, with the Re present in a low positive oxidation state and largely inaccessible to the probe molecule CO.

Here, we summarize results of structural characterization of the sample by extended X-ray absorption fine structure (EXAFS) spectroscopy and hydrogen chemisorption as well as catalytic performance in methylcyclohexane dehydrogenation. Data are included to compare the performance of the model catalysts made from $[Re_2Pt(CO)_{12}]$ with the performance of Pt/γ-Al_2O_3 and Re−Pt/γ-Al_2O_3 catalysts made conventionally from salt precursors.

EXAFS spectroscopy is among the most incisive methods for the characterization of dispersed catalysts that lack long-range order.[3] This technique has been used to characterize the metal−metal interactions in supported bimetallic catalysts, including Re−Pt/γ-Al_2O_3 prepared from salt precursors.[4] The data showed that, after reduction with H_2 at 500 °C, alloy-like Re−Pt particles were present, but the interpretation was limited by the overlap of the Re L_{II} and Pt L_{III} edge data. Furthermore, the analysis did not include any contribution from the metal−support interface, and a k^3 weighting was used in the Fourier transformation (k is the wave vector), making the analysis insensitive to low atomic weight scatterers, such as the oxygen atoms of the support.[5] Caballero *et al.*[6] used *in situ* EXAFS spectroscopy to investigate the effect of hydrocarbon deposits on Pt/γ-Al_2O_3 and on Re−Pt/γ-Al_2O_3 catalysts, detecting a new type of Pt−C bond formation on the bimetallic catalyst under reaction conditions. In their EXAFS analysis, the authors did not attempt to distinguish between Pt−Pt and Pt−Re absorber−backscatterer pairs and did not detect any contribution from the metal−support interface,[7,8] notwithstanding the small average Pt and Re−Pt cluster sizes (the first-shell metal−metal coordination numbers were 4.4 and 3.6, respectively).

[†] University of Delaware.
[‡] E. I. du Pont de Nemours and Company.
[§] Utrecht University.
[⊥] University of California.
[⊗] Abstract published in *Advance ACS Abstracts,* June 1, 1997.

(1) Kluksdahl, H. E. U.S. Patent 3 415 737, 1968.
(2) Fung, A. S.; McDevitt, M. R.; Tooley, P. A.; Kelley, M. J.; Koningsberger, D. C.; Gates, B. C. *J. Catal.* **1993**, *140*, 190.
(3) Prins, R.; Koningsberger, D. C. In *X-ray Absorption: Principles, Applications, Techniques of EXAFS, SEXAFS And XANES;* Koningsberger, D. C., Prins, R., Eds; Wiley: New York, 1988; Chapter 8.
(4) Meitzner, G.; Via, G. H.; Lytle, F. W.; Sinfelt, J. H. *J. Chem. Phys.* **1987**, *87*, 6354.
(5) Koningsberger, D. C. In *Physics and Chemistry of Solids, Hercules Course, Neutron and Synchrotron Radiation for Condensed Matter Studies, Vol. II., Applications to Solid State Physics and Chemistry;* Baruchel, J., Hodeau, J. L., Lehmann, M. S., Regnard, J. R., Schlenker, C., Eds.; Springer: Berlin, 1994; Chapter X, pp 213−244.
(6) Caballero, A.; Villain, F.; Dexpert, H.; Lepeltier, F. *J. Chem. Soc., Faraday Trans.* **1993**, *89*, 159.
(7) Vaarkamp, M.; Modica, F. S.; Miller, J. T.; Koningsberger, D. C. *J. Catal.* **1993**, *144*, 611.
(8) Koningsberger, D. C.; Vaarkamp, M. *Physica B* **1995**, *208 & 209*, 633.

S0002-7863(96)02816-8 CCC: $14.00

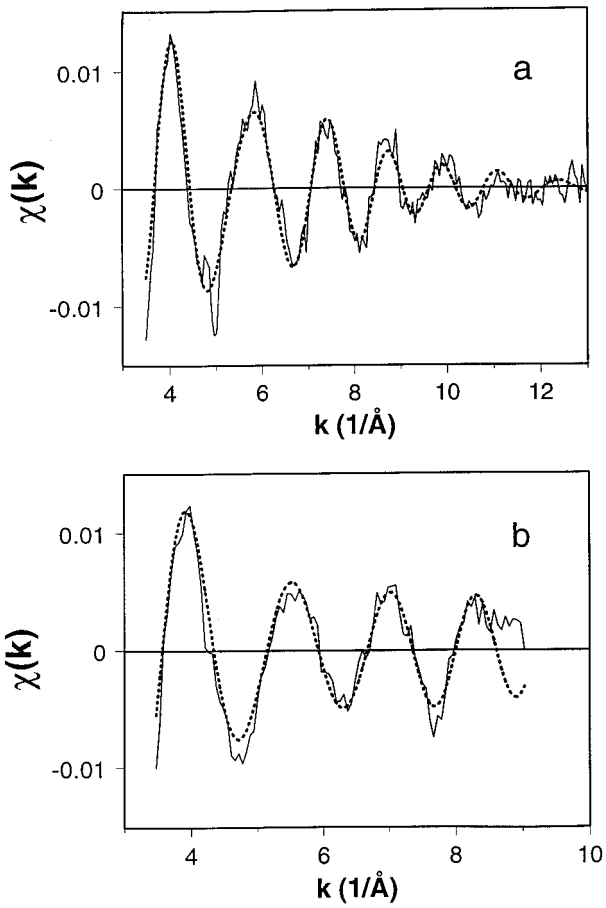

Figure 1. (a) Raw Re EXAFS data (solid line) and k^0 fit (dotted line) and (b) raw Pt EXAFS data (solid line) and k^0 fit (dotted line) obtained after treatment in H_2 of the γ-Al_2O_3-supported sample made by adsorption of $[Re_2Pt(CO)_{12}]$.

Because of the high dispersion of the metal in our catalyst made from $[Re_2Pt(CO)_{12}]$, there was negligible overlap of the Re- and Pt-edge data in the X-ray absorption spectrum. Thus, the sample presented an excellent opportunity to characterize the Re−Pt interactions without neglecting the metal−support contributions in the data analysis. The results demonstrate that Re and Pt backscatterers can be distinguished well, provided that a low k weighting (preferably, a k^0 weighting) is used in the analysis of the EXAFS data.

The catalytic test reaction, dehydrogenation of methylcyclohexane, was chosen because it is a structure-insensitive reaction catalyzed by the metallic function of a reforming catalyst.[9] Because methylcyclohexane is a potential coke precursor,[10] this reaction is appropriate to characterize the deactivation of the metallic function of the catalyst. The conversion of methylcyclohexane proceeds with a high selectivity for toluene formation (although methane and benzene form also[11,12]), giving a simpler product distribution than other commonly used test reactions for characterization of hydrocarbon reforming, e.g., *n*-hexane reforming. Moreover, this reaction involves both the metal and acid functions of the catalyst.

Results

EXAFS Spectroscopy. The raw EXAFS data characterizing the sample made from $[Re_2Pt(CO)_{12}]$ on γ-Al_2O_3 following treatment in H_2 at 400 °C are presented in Figure 1a (Re edge) and Figure 1b (Pt edge). The data represent the sample in the presence of H_2 at nearly liquid nitrogen temperature. Oscillations were completely damped at values of $k > 13$ Å^{-1} beyond the Re L_{III} edge. Consequently, the contribution from the Re EXAFS at the Pt L_{III} edge was less than the noise, allowing the use of standard separate-element methods to analyze the Pt-edge EXAFS function without complicated deconvolution techniques.[4] The quality of the Pt L_{III} edge EXAFS data is satisfactory, although the Pt loading was only 0.56 wt %. The appearance of the Re L_{II} absorption edge at 11959 eV limited the useful range of the Pt EXAFS function to $k < 9$ Å^{-1}.

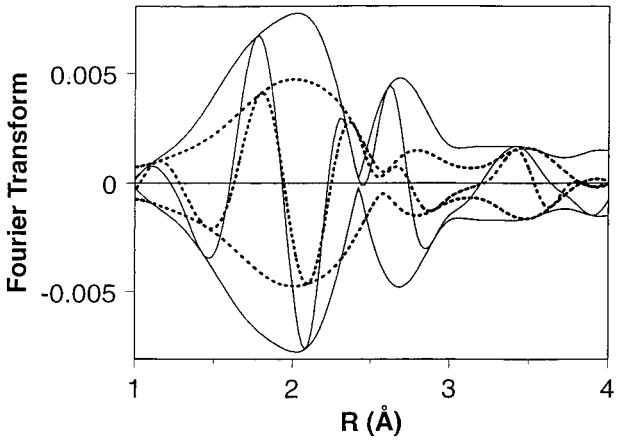

Figure 2. A comparison of the Fourier transforms (k^0, $\Delta k = 3.1-12$ Å^{-1}) of the Re EXAFS of an γ-Al_2O_3-supported sample formed by adsorption of $[Re_2Pt(CO)_{12}]$ (solid line) and the γ-Al_2O_3-supported sample made by adsorption of $[H_3Re_3(CO)_{12}]$ (dotted line), both after treatment in H_2.

Structural results obtained for a sample prepared from $[H_3Re_3(CO)_{12}]$ on γ-Al_2O_3[13] provided a basis for analysis of metal−support interactions in the bimetallic sample. The Re L_{III}-edge EXAFS data characterizing the sample prepared from $[Re_2Pt(CO)_{12}]$ were first compared with the Re L_{III}-edge EXAFS data characterizing the sample prepared from $[H_3Re_3(CO)_{12}]$[13] by a k^0-weighed Fourier transformation (Figure 2). As summarized in the section below entitled EXAFS Data Analysis, a k^0-weighed Fourier transform can distinguish between Pt and Re as neighboring atoms. The Re−O and Re−Re contributions appear in similar radial regions, as indicated by the imaginary part of the Fourier transform. However, an additional contribution was found, in the range $2.4 < r < 2.8$ Å. This contribution is inferred to be an indication of the presence of Pt in the neighborhood of Re, because when only a Re−O and a Re−Re contribution were included in the fit, it was not possible to fit the k^0-weighted Fourier transform in the range $2.4 \leq r \leq 2.8$ Å (where r is the absorber−backscatterer distance). Moreover, in k space the fit starts to deviate from the data at values of $k > 9$ Å^{-1}; the amplitude of the fit is too high, and it is clear that another scatterer has to be included, which has a different enough phase shift to diminish the amplitude of the oscillations at high values of k as a consequence of interference.

On the basis of the assumption that a bimetallic interaction can be detected from both the Re L_{III} and the Pt L_{III} edges, the strategy used in analyzing the EXAFS data for the Re−Pt sample is analogous to the predictor−corrector scheme in numerical analysis; the Re L_{III} edge is the predictor and the Pt L_{III} edge is the corrector. Because a criterion for a satisfactory analysis was that the same values for the distances ($R_{Pt-Re} = R_{Re-Pt}$) and for the disorder ($\Delta\sigma^2_{Pt-Re} = \Delta\sigma^2_{Re-Pt}$) had to be

(9) Jossens, L. W.; Petersen, E. E. *J. Catal.* **1982**, *76*, 265.
(10) Myers, C. G.; Lang, W. H.; Weisz, P. B. *Ind. Eng. Chem.* **1961**, *53*, 299.
(11) Grenoble, D. C. *J. Catal.* **1979**, *56*, 32.
(12) Grenoble, D. C. *J. Catal.* **1979**, *56*, 40.
(13) Fung, A. S.; Tooley, P. A.; Kelley, M. J.; Koningsberger, D. C.; Gates, B. C. *J. Phys. Chem.* **1991**, *95*, 225.

Table 1. Fourier Transform and Analysis Ranges

edge	anal. range[a] Δk (Å^{-1})	used range ΔR (Å)	N_{indp}[b]	ν[c]	noise ampl	ϵ_ν[2 d]
Re	3.5−13	1.0−3.5	16	4	0.002	2.1
Pt	3.5−8.5	1.0−3.5	9	3	0.002	1.5

[a] Weight fit: k^0. [b] N_{indp} is the number of independent points. [c] $\nu = N_{indp} - N_{fit}$. [d] See Report on Standards and Criteria: Lytle, R. W.; Sayers, D. E.; Stern, E. A. *Physica B* **1989**, *158*, 701.

Table 2. EXAFS Coordination Parameters[a]

edge	coordination	N	$10^3\,\Delta\sigma^2$ (Å^2)	R (Å)	ΔE_0 (eV)
Re	Re−Re	2.6(17)	2(4)	2.61(5)	−2(6)
	Re−Pt	0.8(7)	−1(5)	2.74(6)	−4(4)
	Re−O	2.4(8)	13(5)	2.14(3)	−14(3)
Pt	Pt−Re	2.5(5)	−1(*)[b]	2.74(*)[b]	5(3)
	Pt−O	1.5(4)	6(13)	2.69(6)	4(4)

[a] Values in parentheses are standard deviations (in last given digit) calculated from the covariance matrix and the estimates of the noise level in the raw data. [b] Parameter kept fixed.

obtained from both the Re-edge and the Pt-edge data, the Re−Pt distance and the Re−Pt disorder ($\Delta\sigma^2_{Re-Pt}$) estimated in the analysis of the Re data were used as the first guesses for the Pt−Re distance and the Pt−Re disorder, respectively. Table 1 includes details of the Fourier transformation and analysis ranges. A three-shell fit (Re−O, Re−Re, and Re−Pt) in r space (Fourier transform range, $3.5 < k < 13$ Å^{-1}) with k^0 weighting, an r-space window of $1 < r < 3.5$ Å, and 12 free parameters resulted immediately in a set of coordination parameters nearly the same as the values presented in Table 2. The Pt EXAFS data were also analyzed by using a k^0-weighted fit in r space with the window $1 < r < 4$ Å and a Fourier transform range of $3.5 < k < 8.5$ Å^{-1}.

Several structural models were used to guide the fitting of the Pt-edge EXAFS data; they included the following contributions, respectively: (1) Pt−Pt + Pt−Re, (2) Pt−Pt + Pt−Re + Pt−O, and (3) Pt−Re + Pt−O. The only structural model which led both to acceptable coordination parameters and to an acceptable goodness of fit was that including only a Pt−Re and a Pt−O coordination. Remarkably, the fit based on this model gave approximately the same values for the Pt−Re distance and the Pt−Re disorder term ($\Delta\sigma^2$) as were obtained from the first fit results obtained for the Re-edge data. With the optimized structural parameters obtained from the Pt EXAFS data, the coordination parameters characterizing the Pt edge were further refined until consistent results were obtained from the analysis of both sets of data. The final fits in k space for the Re and the Pt EXAFS are indicated with dotted lines in Figure 1, parts a and b, respectively.

The individual Re−Re, Re−Pt, and Re−O contributions, which constitute the total Re EXAFS signal, are plotted in Figure 3a. The Re−Pt and Re−Re EXAFS signals at values of $k >$ 10 Å^{-1} are opposite in phase, which explains the rapid damping of the total EXAFS signal at values of k in this range. Inclusion of a Re−Pt contribution in the Re EXAFS data analysis was therefore necessary to give a good fit in this range of k. Figure 3a also shows that the Re−O contribution is dominant at low values of k; thus this contribution cannot be ignored in the analysis.

The individual Pt−Re and Pt−O EXAFS contributions are shown in Figure 3b. The results show that the Pt−O contribution is large at low values of k, which again explains the importance of using a k^0 weighting in the analysis. The agreement between the Fourier transforms of each individual contribution and the Fourier transforms of the corresponding

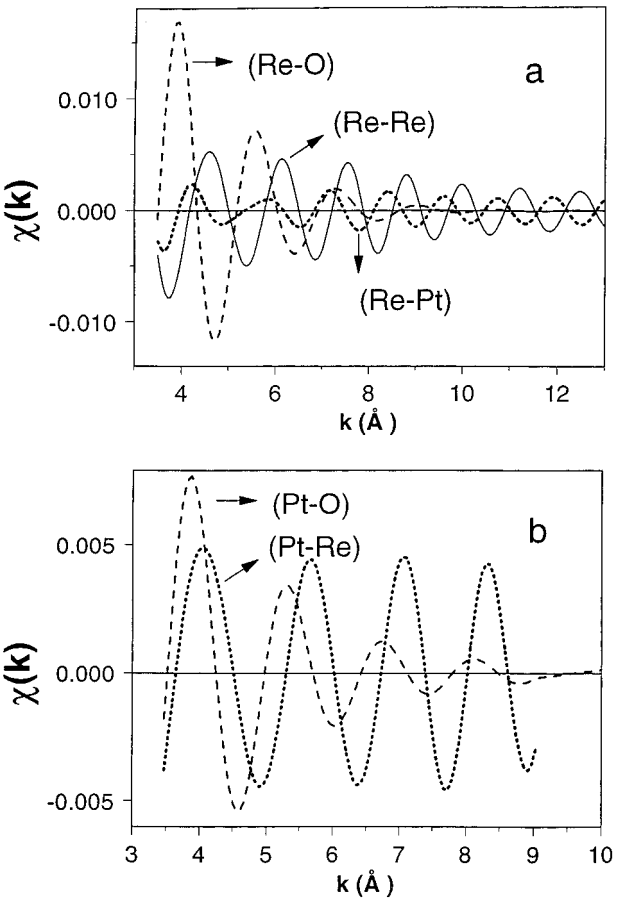

Figure 3. EXAFS data characterizing the sample prepared from $[Re_2Pt(CO)_{12}]$ on γ-Al_2O_3 following treatment in H_2 with individual contributions obtained from the fitting procedure: (a) Re-Re (solid line), Re−Pt (dotted line), and Re−O (dashed line) and (b) Pt−Re (dotted line) and Pt−O (dashed line).

difference files are shown for the Re and Pt EXAFS analyses in Figures 4 and 5, respectively.

Table 1 includes further details of the fitting procedure and the final goodness of fit values. The coordination parameters obtained in the analysis are given in Table 2. The values in brackets, determined in a statistical analysis of the data, indicate the limits of precision given in the last digit of the values of the coordination parameters. In the statistical analysis of the Pt EXAFS data, the coordination distance and disorder of the Pt−Re coordination were not allowed to vary and were kept equal to the values obtained for the same coordination analyzed from the Re EXAFS data. This method allowed the statistical analysis of the Pt EXAFS data, which were obtained over only a small range of values of k, limiting the degrees of freedom in the fitting.

Hydrogen Chemisorption. The hydrogen chemisorption results show that Pt/γ-Al_2O_3 dried at 120 °C in He followed by reduction in H_2 at 500 °C had a H/Pt ratio (atomic) of 0.92, whereas Pt/γ-Al_2O_3 dried in He at 500 °C followed by reduction in H_2 at 500 °C had a lower fraction of the metal atoms exposed, as indicated by a H/Pt ratio (atomic) of 0.51. The treatment conditions stated here match those used in the catalysis experiments.

Catalyst Performance. The catalysis experiments were carried out to provide a comparison of the performance of the $[Re_2Pt(CO)_{12}]$-derived catalyst with those of conventional salt-derived catalysts; two of the latter (without Re) were prepared to have different fractional exposures of Pt by variations in the

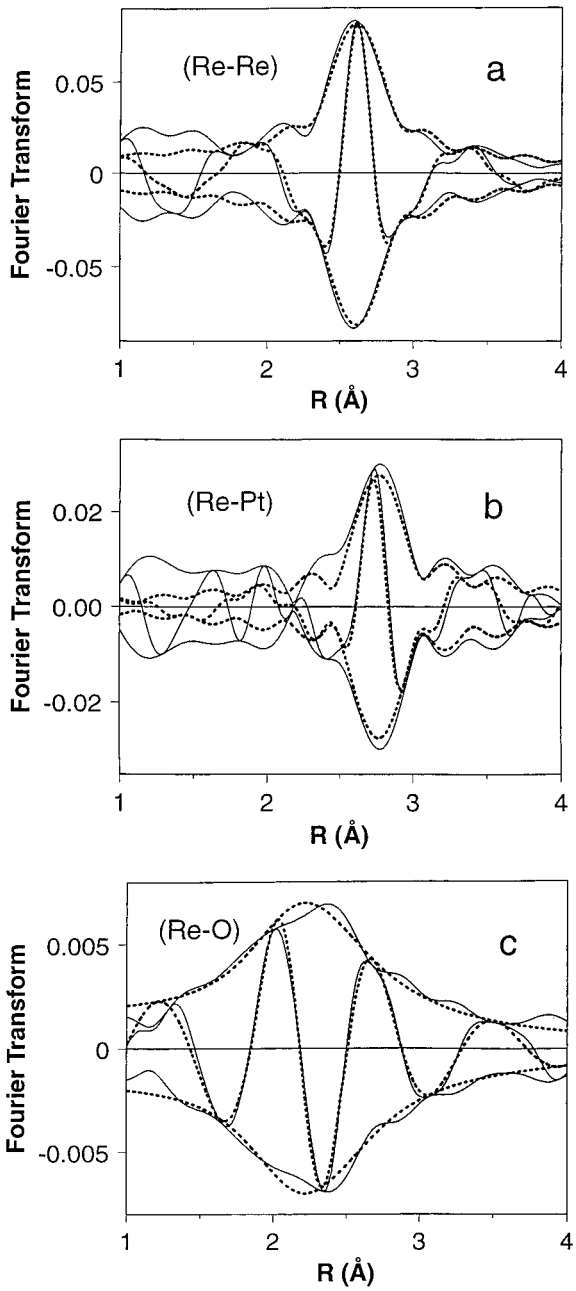

Figure 4. EXAFS data characterizing the sample prepared from $[Re_2Pt(CO)_{12}]$ on γ-Al_2O_3 following treatment in H_2. Fourier transform (k^0, $\Delta k = 3.5-13$ Å^{-1}) of difference files and calculated contributions; (a) Re−Re, raw Re EXAFS minus [(Re−Pt) + (Re−O)] (solid line) and calculated Re−Re contribution (dotted line) (Fourier transform, FT, is Re−Re phase and amplitude corrected); (b) Re−Pt, raw Re EXAFS minus [(Re−Re) + (Re−O)] (solid line) and calculated Re−Pt contribution (dotted line) (FT is Re−Pt phase and amplitude corrected); and (c) Re−O, raw Re EXAFS minus [(Re−Re) + (Re−Pt)] (solid line) and calculated Re−O contribution (dotted line) (FT is Re−O phase corrected).

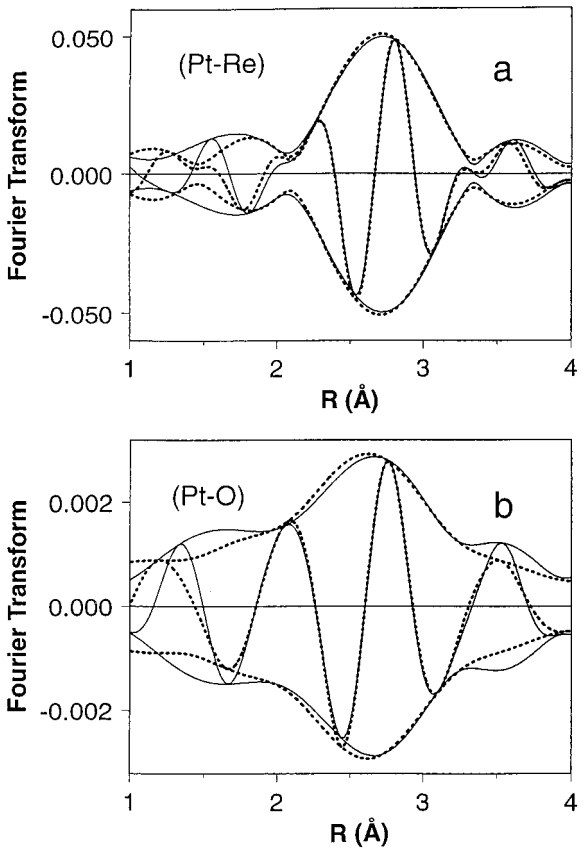

Figure 5. EXAFS data characterizing the sample prepared from $[Re_2Pt(CO)_{12}]$ on γ-Al_2O_3 following treatment in H_2. Fourier transform (k^0, $\Delta k = 3.5-8.5$ Å^{-1}) of difference files and calculated contributions: (a) Pt−O, raw Pt EXAFS minus (Pt−O) (solid line) and calculated Pt−Re contribution (dotted line) (FT is Pt−Re phase and amplitude corrected) and (b) Pt−Re, raw Pt EXAFS minus (Pt−Re) (solid line) and calculated Pt−O contribution (dotted line) (FT is Pt−O phase corrected).

conditions of treatment (drying and reduction), as stated in the preceding paragraph; a third salt-derived catalyst contained both Re and Pt.

Under the conditions of these experiments, each catalyst was characterized by a high initial conversion, >90%. The results of the catalytic reaction experiments do not provide a meaningful discrimination of the catalysts on the basis of initial activities. Rather, they indicate clear distinctions with regard to catalyst stability. The conversion of methylcyclohexane observed with each catalyst decreased with time on stream in the flow reactor (Figure 6). The $[Re_2Pt(CO)_{12}]$-derived catalyst was the most resistant to deactivation; after 40 h on stream, it was markedly more active than the other catalysts. Of the two Pt/γ-Al_2O_3 catalysts, the one with the higher fractional exposure of Pt was the more resistant to deactivation.

The catalysts were similar to each other in their selectivities. The selectivity for dehydrogenation, measured by the yield of toluene (defined as moles of toluene formed/mole of methylcyclohexane converted) as a function of time on stream, is shown in Figure 7. Each catalyst was characterized by an induction period of about 20 h, after which the yield of toluene was about 90%.

The data are accurate enough to provide only partial information regarding the minor products. The hydrodealkylation conversion is indicated by the fraction of methane and the fraction of benzene in the product stream. The product analyses for methane were more accurate than those for benzene, and thus the former are taken as the best indication of the selectivity for toluene dealkylation.[11,12] The results agree qualitatively with those reported by Jossens and Petersen[9] with regard to the selectivities for dehydrogenation and hydrodealkylation of methylcyclohexane by γ-Al_2O_3-supported Re−Pt and Pt catalysts prepared from salt precursors.

The treatment conditions influencing Pt crystallite growth during activation of salt-derived Pt/Al_2O_3 catalysts affect the

(14) Ruckenstein, E. In *Metal−Support Interactions in Catalysis, Sintering and Redispersion*; Stevenson, S. A., Dumesic, J. A., Baker, R. T. K., Ruckenstein, E., Eds.; Van Nostrand Reinhold: New York, 1987; p 141.

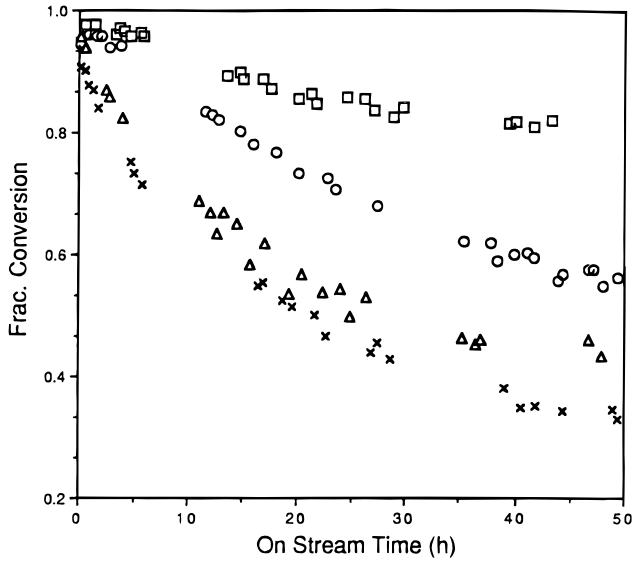

Figure 6. Conversion of methylcyclohexane and H_2 catalyzed by γ-Al_2O_3-supported Pt and Re−Pt catalysts at 1 atm and 400 °C. Comparison of the deactivation rates of several catalysts containing supported Pt. Symbols: □, catalyst prepared from $[Re_2Pt(CO)_{12}]$; △, catalyst prepared from Re and Pt salt precursors; ○, catalyst prepared from Pt salt precursor and treated at 120 °C; ×, catalyst prepared from Pt salt precursor and treated at 500 °C.

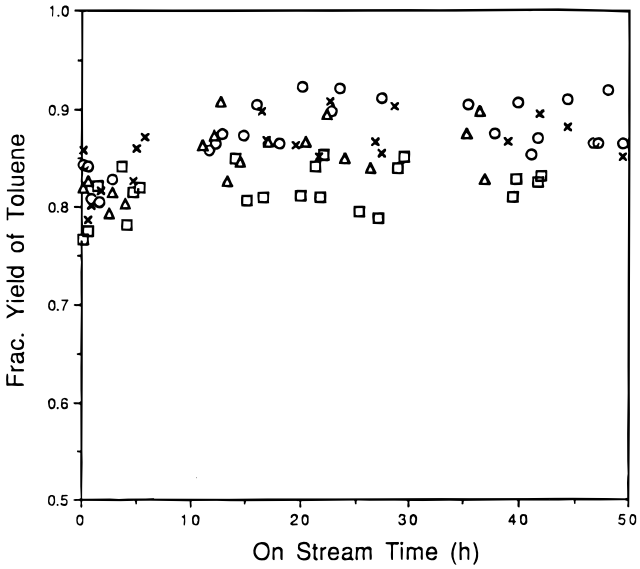

Figure 7. Toluene formation in the dehydrogenation of methylcyclohexane at 400 °C and 1 atm in the presence of γ-Al_2O_3-supported Pt and Re−Pt catalysts. The ordinate represents the fraction of the converted methylcyclohexane that was converted into toluene. The symbols are defined in the caption of Figure 6.

rate of catalyst deactivation.[14−17] The generation of moisture during the reduction of PtO_2 to give Pt at high temperatures weakens the interaction between Pt and the support and increases the rate of Pt migration and sintering.[18] Thus an experiment was done to test for a change in the fraction of Pt exposed as a result of Pt sintering during the catalyst preparation. In one of the preparations, the He flow was switched to H_2 flow at high temperature during the activation of a Pt/γ-Al_2O_3 catalyst. After drying at 500 °C in He, the Pt/γ-Al_2O_3 catalyst was cooled to room temperature in He, and instead of beginning H_2 flow to replace He after a temperature of 500 °C had been reached, the H_2 flow was maintained during the entire heating process, as the temperature was ramped to 500 °C. After continued treatment in H_2 at 500 °C for 4 h, the catalyst was subjected to the same reaction conditions for methylcyclohexane dehydrogenation as the Pt catalyst with a lower fractional exposure of Pt, which had been dried at 120 °C in He followed by treatment in H_2 500 °C.

The rates of deactivation of these two catalysts were different (Figure 6); these results suggested that the fractional exposure of the Pt (which was influenced by the sintering) was important in determining the rate of catalyst deactivation.

Discussion

Distinguishing Pt and Re Scatterers in the Presence of Low-Z Scatterers. The results of the EXAFS data analysis show that it is possible to distinguish between Re and Pt as backscattering atoms, provided that no *k* weighting is used in the analysis. It is immediately clear from Figure 3, parts a and b, that inclusion of Re−O and Pt−O contributions from the support is necessary to obtain a satisfactory analysis of the Re and Pt EXAFS data characterizing the sample prepared from $[Re_2Pt(CO)_{12}]$. Metal−support contributions can be detected only if these contributions are a large enough part of the total EXAFS spectrum, i.e., only if the metal particles or clusters are small enough.[19,20] The fact that it was possible to obtain a good fit of the data by using only first-shell metal−metal and metal−oxygen contributions is also a strong indication that the bimetallic clusters in the sample consisted of only a few metal atoms.

Structural Model of Supported Pt−Re Clusters. The EXAFS data provide the basis for a structural model of the supported bimetallic clusters, as follows. Analysis of the Pt L_{III}-edge EXAFS data shows that there were only Re and O neighbors around each Pt atom, with an average Pt−Re distance of 2.74 Å and an average Pt−Re coordination number of 2.5 (any hydrogen backscatterers were not detected in the EXAFS analysis). Analysis of the Re L_{III}-edge EXAFS data resulted in an average Re−Pt coordination number of 0.8. The average Re−Re coordination number was 2.6. The Pt−support interface is characterized by a Pt−O coordination number of 1.5 with a distance of 2.69 Å. The Re−support interface is characterized by a Re−O coordination number of 2.4 with a distance of 2.14 Å.

These data form the basis for a structural model of the supported bimetallic species, but because the coordination numbers and distances are averaged over all the different types of coordinations present, the structural model is simplified. The model is shown in Figure 8; it does not account for any hydrogen present. The coordination numbers representing the model are compared in Table 3 with the values determined in the EXAFS analysis. The agreement is good. The model implies that two Re_2Pt moieties originating from the $[Re_2Pt(CO)_{12}]$ precursor were the building blocks of the average supported bimetallic cluster, which is represented as approximately Re_4Pt_2. We stress that this model represents the catalyst in the presence of H_2 at nearly liquid nitrogen temperature in a state prior to application;

(15) Ruckenstein, E. In *Sintering and Heterogeneous Catalysis*, Kuczynski, G. C.; Miller, A. E.; Sargent, G. A., Eds.; Plenum: New York, 1983; p 199.
(16) Wanke, S. E. In *Sintering and Heterogeneous Catalysis*; Kuczynski, G. C., Miller, A. E., Sargent, G. A., Eds.; Plenum: New York, 1983; p 223.
(17) Wanke, S. E.; Szymura, J. A.; Yu, T. T. In *Catalyst Deactivation*; Petersen, E. E., Bell, A. T., Eds.; Marcel Dekker: New York, 1987; p 65.
(18) Chu, Y. F.; Ruckenstein, E. *J. Catal.* **1978**, *55*, 281.
(19) Koningsberger, D. C.; Gates, B. C. *Catal. Lett.* **1992**, *14*, 271.
(20) van Zon, F. B. M.; Maloney, S. D.; Gates, B. C.; Koningsberger, D. C. *J. Am. Chem. Soc.* **1993**, *115*, 10317.

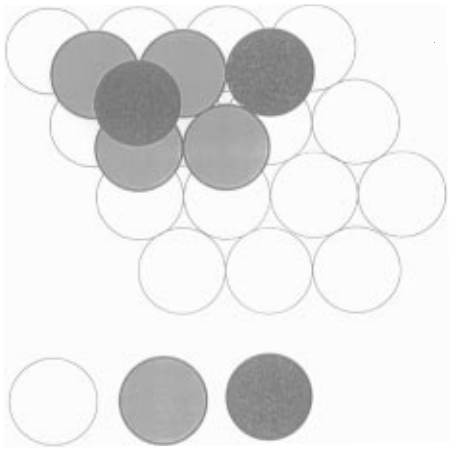

Figure 8. Structural model of Re_4Pt_2 clusters on γ-Al_2O_3 based on the coordination parameters obtained from the Re L_{III} and Pt L_{III} edge EXAFS analyses. The clusters are presumed to reside in registry with the [111] surface of γ-Al_2O_3.

Table 3. Comparison of Coordination Numbers *N* Characterizing EXAFS Data Analysis and Structural Model

	N	
coordination	EXAFS	model
Re−Re	2.6	2.5
Re−Pt	0.8	1.25
Re−O	2.4	3.0
Pt−Re	2.5	2.5
Pt−O	1.5	1.5

under catalytic reaction conditions, the structure was likely modified by the reactants.

The Re−O and Pt−O coordination numbers are crucial parameters for the structural model. The average Pt−O and Re−O coordination numbers *N* obtained from the EXAFS data analysis ($N_{Pt-O} = 1.5$, $N_{Re-O} = 2.4$) can be explained only by a model in which the Re−Pt cluster has a [111] epitaxy in registry with the [111] surface planes of the γ-Al_2O_3 support. This arrangement corresponds to a layer of Re atoms that are all in contact with the support, with each Re atom positioned in a 3-fold hollow site, corresponding to an average Re−O coordination number of 3. Within the expected limits of accuracy of the experimental Re−O coordination number determined in the EXAFS analysis, this value (2.4) is indistinguishable from the value of 3 corresponding to the model. The average Pt−O coordination number of 1.5 is accounted for if (1) one Pt atom is placed in a 3-fold hollow site, thus having three oxygen neighbors of the support, and (2) if the second Pt atom is coordinated only to Re atoms and is positioned on top of the layer of Re atoms (Figure 8).

The suggestion that the clusters reside on the [111] surface of γ-Al_2O_3 is consistent with the surface chemistry of γ-Al_2O_3 powder. The [111] surface plane of γ-Al_2O_3 is not the only plane exposed by powder γ-Al_2O_3, but it is stable and has been suggested on the basis of electron diffraction and electron microscopy[21−23] to be the predominant surface. Consistent with the structural hypothesis, the metal−support interface structures of Rh/γ-Al_2O_3[24] and Ir/γ-Al_2O_3[25] determined from EXAFS data are consistent with the assumption that the metal particles are preferentially positioned on the [111] surface planes of the support. Additional EXAFS evidence of a [111] epitaxy has been obtained for Pt/γ-Al_2O_3, for which the formation of the metal−support interface was followed as a function of the reduction temperature.[26]

Characterization of the sample made from $[Re_2Pt(CO)_{12}]$ by X-ray photoelectron spectroscopy and threshold resonance experiments[2] indicated the presence of Re in a low positive oxidation state. This low-valent form has an average Re−Re distance of 2.61 Å, determined by the EXAFS data, which is 0.13 Å less than the value for bulk Re metal. A short Re−Re distance of 2.67 Å was also determined by EXAFS analysis for γ-Al_2O_3-supported clusters formed from $[H_3Re_3(CO)_{12}]$ after treatment in H_2.[13] X-ray photoelectron spectroscopy also indicated a low, non-zero oxidation state of Re in this sample,[2] which was modeled as trirhenium rafts on the surface of γ-Al_2O_3.[13]

Metal−metal distances in small supported clusters of noble metals are contracted relative to those of the bulk metal.[27−29] Theoretical calculations[30] show that a contraction of the metal−metal distance with decreasing cluster size is a consequence of a decrease in the delocalization energy, which leads to a higher charge density between the metal atoms. This leads to a better screening of the nuclei, resulting in a shortened metal−metal distance. However, the EXAFS experiments described in this paper were carried out with samples in the presence of chemisorbed hydrogen. Chemisorption of hydrogen leads to withdrawal of electron density from the metal atoms[29] and therefore tends to cancel the effect of decreasing the delocalization energy; in the presence of chemisorbed hydrogen[29,31] the metal−metal distance relaxes back to values nearly equal to those observed for bulk noble metals. Thus, the short Re−Re distance of 2.61 Å observed here for the Re−Pt clusters in the presence of chemisorbed hydrogen can only be explained by the positive oxidation state of the oxophilic Re, consistent with the X-ray photoelectron spectra.

The 2.14-Å Re−O distance is in close agreement with the metal−oxygen distances characterizing the metal−support interface in reduced γ-Al_2O_3- and KLTL zeolite-supported Pt catalysts after reduction at high temperatures (≥450 °C)[7,8] and is regarded as a bonding distance characteristic of oxygen ions interacting with cations in low oxidation states.[32] In contrast, the 2.69-Å Pt−O distance is typical of the metal−oxygen distances observed in noble metal−metal oxide support interfaces in which atomic (chemisorbed) hydrogen is present[7,8,20,24] and which have been reduced at temperatures in the range of 300 to 450 °C. Reduction at high temperatures (≥450 °C)[7,8] or evacuation at 350 °C after low-temperature (300 °C) reduction[31] leads to the disappearance of this long metal−oxygen

(21) Lippens, B. C.; de Boer, J. H. *Acta Crystallogr*. **1964**, *17*, 1312.
(22) Iijima, S. *Jpn. J. Appl. Phys.* **1984**, *23*, L347.
(23) Iijima, S. *Surf. Sci*. **1985**, *156*, 1003.
(24) van Zon, J. B. A. D.; Koningsberger, D. C.; van't Blik, H. F. J.; Sayers, D. E. *J. Chem. Phys.* **1985**, *82*, 5742.
(25) van Zon, F. B. M.; Visser, G. J.; Koningsberger, D. C. *Proceedings of the International Congress on Catalysis (Calgary)*; Phillips, M. J., Ternan, M. J., Eds.; The Chemical Institution of Canada: Ottawa, 1988; Vol. 3, p 1386.
(26) Muñoz Paez, A.; Koningsberger, D. C. *J. Phys. Chem.* **1994**, *99*, 4193.
(27) Moraweck, B.; Renouprez, A. J. *Surf. Sci.* **1981**, *106*, 35.
(28) van't Blik, H. F. J.; van Zon, J. B. A. D.; Koningsberger, D. C.; Prins, R. *J. Mol. Catal.* **1984**, *25*, 379.
(29) Vaarkamp, M.; Koningsberger, D. C. *J. Phys. Chem*. Submitted for publication.
(30) Delley, B.; Ellis, D. E.; Freeman, A. J.; Baerends, E. J.; Post, D. *Phys. Rev. B.* **1983**, *27*, 2132.
(31) Koningsberger, D. C.; Vaarkamp, M.; Muñoz Paez, A.; van Zon, F. B. M.; *X-ray absorption fine structure for catalysts and surfaces*; Iwasawa, Y., Ed.; 1995; Series on Synchrotron Radiation Techniques and Applications, Vol. 2.
(32) Chang, J.-R.; Gron, L. U.; Honji, A.; Sanchez, K. M.; Gates, B. C. *J. Phys. Chem.* **1991**, *95*, 9944.

distance and results in a direct contact of the interfacial metal atoms with the support oxygen ions at a distance of about 2.1 or 2.2 Å, which is a metal ion−oxygen bonding distance.[32] Readsorption of hydrogen at room temperature after evacuation at low temperatures restores the metal−oxygen distance of about 2.7 Å.[31] The differences between the Re−O and the Pt−O distances observed after reduction at 400 °C with the sample measured in the presence of H_2 are inferred to result from the oxophilic nature of Re, favoring its coordination with oxygen, while atomic hydrogen could still be present between the Pt and its oxygen neighbors of the support.

The structural model of Figure 8 is consistent with all the available characterization data. For example, infrared spectra[2] indicated the lack of adsorption of NO or CO on Re in the bimetallic sample made from $[Re_2Pt(CO)_{12}]$. The absence of these adsorbates on the Re led to the suggestion that nearby Pt blocked adsorption on Re. This suggestion is consistent with the structural model, whereby one Pt atom lies atop the Re monolayer, covering the Re atoms, and the other Pt atom is in direct contact with the support and also directly accessible for adsorption.

The intimacy of Pt and Re in this novel structure presumably makes the reduction of Re more facile than that in a sample prepared from the separate precursors $[H_3Re_3(CO)_{12}]$ and $[Me_2Pt(COD)]$; the latter demonstrated no difference in its reducibility of Re by H_2 relative to that of a monometallic Re sample.[2] We conclude that the Pt and Re in the latter sample were not in intimate contact.

Thus, in the catalyst made from $[Re_2Pt(CO)_{12}]$, Re exists at the interface between Pt and the Al_2O_3 surface, and its oxophilicity may promote a strong bonding of the clusters to the Al_2O_3 surface. Electron-deficient Re is expected to be more strongly bonded to the support than metallic Re. Since Pt is stably bonded to Re in the bimetallic structure, we suggest that low-valent Re cations are better ligands for Pt than the available alternatives. The small cluster size also allows the exposure of Re and Pt to O_2 during passivation in a temperature-programmed oxidation, resulting in the oxidation of metallic Pt to Pt^{2+} and of low-valent Re to Re^{6+} or Re^{7+}, as was observed.[2] The low temperature for the maximum rate of reduction of the passivated cluster-derived Pt−Re sample also confirms the relative intimacy of Re and Pt.

The structural model of Figure 8 does not closely resemble any known molecular analogue, but it makes good chemical sense in that the oxophilic Re is coordinated to as many oxygen atoms of the support as possible (assuming the [111] face of the γ-Al_2O_3), and the Pt atoms are as highly coordinated as possible given the arrangement of Re atoms indicated by the EXAFS data. We suggest that structures similar to those of the model formed on the support surface as a result of decarbonylation of the precursor formed from $[Re_2Pt(CO)_{12}]$ by treatment in H_2 at 400 °C and that these surface species are quite stable. Because the model is based on EXAFS data determined near liquid nitrogen temperature, it is not known how closely the structures present during catalysis or chemisorption resemble the model.

In summary, we conclude that the proposed structural model representing the sample prepared from $[Re_2Pt(CO)_{12}]$ on γ-Al_2O_3 is consistent with the results of all the physical characterization data. We emphasize, however, that because EXAFS spectroscopy gives only average structural information, the bimetallic cluster proposed in Figure 8 is not expected to be unique. It seems likely that other small bimetallic clusters having similar structural characteristics but containing fewer or more Re and Pt atoms exist in a mixture of surface species.

Structural characteristics similar to those of the clusters on γ-Al_2O_3 formed from $[Re_2Pt(CO)_{12}]$ in this work have been attributed to other bimetallic naphtha reforming catalysts, such as Al_2O_3-supported Ir−Pt and Sn−Pt. On the basis of EXAFS results, Sinfelt *et al.*[33] suggested the formation of Al_2O_3-supported Ir−Pt particles smaller than about 20 Å in diameter, if they are assumed to be spherical. Surface enrichment of Pt occurs as a consequence of the difference in surface energies of Ir and Pt, and the authors suggested that the particles may not be spherical, but rather may be rafts with a ring of Pt atoms around the perimeter. The model of our Re−Pt clusters formed from $[Re_2Pt(CO)_{12}]$ can also be described as raft-like.

This type of bimetallic structure has also been inferred for Al_2O_3-supported Sn−Pt catalysts on the basis of EXAFS spectra, indicating that Pt is highly dispersed atop Sn cations on the Al_2O_3 support.[34] Adkins and Davis[35] and Sexton and Hughes[36] inferred from X-ray photoelectron spectra that Sn was present in a cationic form in monolayers on the Al_2O_3 support, with Pt dispersed on the Sn. Thus these examples of Al_2O_3-supported Ir−Pt and Sn−Pt catalysts indicate that bilayer-like structures may be quite general for highly dispersed M−Pt/Al_2O_3, where M is an oxophilic metal or even the more noble Ir. The structural characteristics of these various bimetallic reforming catalysts may account in part for their stability advantages over simple supported Pt catalysts in commercial operations for naphtha reforming.

Catalyst Performance. The rate of deactivation of the $[Re_2Pt(CO)_{12}]$-derived catalyst was less than the rates of deactivation of the other catalysts investigated in this work. The strong resistance of the bimetallic catalyst to deactivation is consistent with the suggestion based on physical characterization data[2,37] that the Re plays a structural role that stabilizes the dispersion of the Pt and prolongs its catalytic activity; thus, we infer that the structure of the working catalyst bore some resemblance to that of the model shown in Figure 8, whereby a platform of Re stabilizes the dispersed Pt.

These results and the observations mentioned above indicating that changes in the treatment conditions affecting the fractional exposure of Pt influenced the deactivation rate lead us to infer that the fractional exposure of the Pt (which is related to the Pt cluster or crystallite size) may account in large measure for the different rates of deactivation of the several catalysts. γ-Al_2O_3-supported Pt catalysts with various fractional exposures of Pt have been examined by Barbier et al.,[38] who suggested that carbonaceous deposit (coke) formation, which causes deactivation, is influenced by the Pt cluster or crystallite size. Coke content was found to be low in highly dispersed catalysts, and the result has been explained by the inhibition of the polymerization of adsorbed dienes, which requires large metal ensembles. This proposition is consistent with the observation of Davis and Somorjai[40] that carbon is deposited more easily on planes than on edges or corners of Pt single crystals.

Thus, we proceed from the working hypothesis that the observed differences in the rates of deactivation of the several supported metal catalysts investigated in this work may be principally a consequence of the different numbers of initial Pt surface sites among the samples. To test the consistency of

(33) Sinfelt, J. H.; Via, G. H.; Lytle, F. W. *J. Phys. Chem.* **1982**, *76*, 2779.
(34) Meitzner, G.; Via, G. H.; Lytle, F. W.; Fung, S. C.; Sinfelt, J. H. *J. Phys. Chem.* **1988**, *92*, 2925.
(35) Adkins, S. R.; Davis, B. H. *J. Catal.* **1984**, *89*, 371.
(36) Sexton, B. A.; Hughes, A. E. *J. Catal.* **1984**, *88*, 466.
(37) Fung, A. S. Ph.D. Dissertation, University of Delaware, 1989, Chapter 6.
(38) (a) Barbier, J.; Corro, G.; Zhang, Y.; Bournonville, J. P.; Franck, J. P. *Appl. Catal.* **1985**, *13*, 245. (b) Barbier, J. *Appl. Catal.* **1986**, *23*, 225.

Table 4. Parameters Estimated from the Catalyst Deactivation Data

catalyst	$k_0A_1\tau$	k_dA_2, h^{-1}
Pt/γ-Al_2O_3, salt derived[a]	1.95	0.019
Pt/γ-Al_2O_3, salt derived[b]	1.08	0.021
Re−Pt/γ-Al_2O_3, salt derived	1.24	0.020
Re−Pt/γ-Al_2O_3, $[Re_2Pt(CO)_{12}]$ derived	2.56	0.011

[a] Sample dried at 120 °C and then reduced; see text. [b] Sample treated at 500 °C in He for 1 h followed by reduction in H_2 at 500 °C; see text.

the data with this hypothesis, we compare the data with a simple model relating the rates of deactivation of the catalysts to the initial numbers of exposed Pt sites. According to this kinetics model (details are presented elsewhere[37]), the methylcyclohexane conversion is described by two separable functions, one proportional to the exposed Pt surface area and the other a measure of the decay rate constant and the number of active sites for coke formation.

The model is formulated as follows: The rate expression for the dehydrogenation of methylcyclohexane is

$$-\mathrm{d}[P_\mathrm{m}]/\mathrm{d}\tau = k_0A_1a[P_\mathrm{m}] \quad (1)$$

$$-\mathrm{d}a/\mathrm{d}t = k_dA_2a \quad (2)$$

where a is the activity factor related to coke formation, P_m is the partial pressure of methylcyclohexane in the reactant stream, τ is the contact time, t is the on stream time, k_0 is the rate constant for the dehydrogenation reaction, and k_d is the decay rate constant. Surface areas of exposed metal and of active sites for coke formation (probably acid sites) are represented as A_1 and A_2, respectively.

Several assumptions are implicit in this rate expression: The methylcyclohexane conversion is assumed to be catalyzed by Pt only in the catalysts, and the rate of dehydrogenation is assumed to be independent of the H_2 partial pressure and first order in methylcyclohexane. Furthermore, for simplicity, the exponent of a is assumed to be one.

Integrating eq 2 from on stream time 0 to t leads to the following expression for the activity factor a:

$$a = \exp\{-k_dA_2t\} \quad (3)$$

Substitution of eq 3 into eq 1 followed by integration gives an expression in terms of the inlet partial pressure, $P_\mathrm{m}{}^0$, and outlet partial pressure, P_m, of methylcyclohexane. Data that are consistent with the model are expected to fall near a linear plot indicated by the following equation:

$$\ln\{-\ln[P_\mathrm{m}/P_\mathrm{m}{}^0]\} = \ln\{k_0A_1\tau\} - \{k_dA_2\}t \quad (4)$$

Since dehydrogenation of methylcyclohexane is structure insensitive and the reactor was operated with a constant space velocity, k_0 and τ should be the same for all catalysts. Therefore, the only variable in the ordinate intercept of eq 4 is the surface area of the exposed metal, A_1, which is related to the metal dispersion for a given metal loading. The slope of the plot of the appropriate variables (shown elsewhere[37]) is a function of k_d and A_2 and is related to the catalyst deactivation.

The initial conversion data for each catalyst were not used in the plots because of the induction period and because at the initial high conversions the reaction came close to equilibrium. The data were linearly regressed from on stream time 15 to 50 h. The fit to the simple model is good.[37] The parameter values are summarized in Table 4.

To examine whether the intercept of the linear plot suggested by eq 4 is a function of the exposed metal surface area, A_1, the fractional exposure of Pt of the two γ-Al_2O_3-supported catalysts from the same batch after the activation procedures was measured by H_2 chemisorption. The H/M value of each Pt catalyst was converted to metal dispersion by the correlation determined by Kip et al.,[39] which is based on the assumption that the metal clusters were hemispherical. The two γ-Al_2O_3-supported Pt catalysts with the same Pt loading have fractional Pt exposures of 0.85 (H/M = 0.92) and 0.54 (H/M = 0.51). The ratio of the Pt surface areas estimated from the catalysis data plotted as suggested by eq 4 for these two supported Pt catalysts (that dried at 120 °C and that dried at 500 °C) was determined to be 1.8,[37] and their metal dispersion ratio was found by hydrogen chemisorption to be 1.6. Within the limit of accuracy of the chemisorption and reaction experiments, the ratio of the ordinate intercepts is in good agreement with the ratio of exposed metal areas. This agreement suggests the appropriateness of the assumptions underlying the simple model presented here.

The value of $k_0A_1\tau$ characteristic of the $[Re_2Pt(CO)_{12}]$-derived catalyst (Table 4) is greater than the corresponding values characteristic of the other catalysts. This result implies that the $[Re_2Pt(CO)_{12}]$-derived catalyst had the maximum number of exposed and catalytically active metal atoms. This inference is in agreement with a structural model in which Pt is located on top of the Re monolayer with 100% dispersion.

The Re−Pt salt-derived catalyst is characterized by a smaller value of $k_0A_1\tau$ than the $[Re_2Pt(CO)_{12}]$-derived catalyst (Table 4). Thus, consistent with the above interpretation, we infer that the former had fewer catalytically active metal atoms exposed than the latter.

The values of k_dA_2 characterizing the two Pt salt-derived catalysts and the Re−Pt salt-derived catalyst (Table 4) are almost identical [$(2.0 \pm 0.1) \times 10^{-2}$ h^{-1}]. As A_2 is expected to be the same for all the catalysts because the same kind of γ-Al_2O_3 support was used for all, the agreement indicates that the number of active sites for coke formation and the decay rate constant were approximately the same for all three. This is not a surprising result for the salt-derived Re−Pt catalyst because Re and Pt were determined to be mostly segregated, as indicated by EXAFS spectroscopy for a similar catalyst prepared by the same methods but with a slightly higher metal loading.[37] Furthermore, the close agreement in these values for the three salt-derived catalysts supports the assumption that the exponent of a in eqs 1 and 2 is nearly unity.

The value of k_dA_2 characteristic of the $[Re_2Pt(CO)_{12}]$-derived catalyst (Table 4) was found to be a factor of about 2 smaller than that characterizing the salt-derived catalysts. By this measure, the catalyst derived from $[Re_2Pt(CO)_{12}]$ is about twice as stable as the others.

A hypothesis to account for the deactivation of the metal sites in the catalysts is the migration of coke (or its precursors) from the support to the metal surface. If the activity factor (a) is treated as a function to account for the decrease in exposed metal surface area with respect to on stream time caused by coke accumulation, the decay rate constant k_d can be viewed as a term to describe the rate of coke migration from the support to the exposed metal surface. Alternatively, the decay rate constant might be speculated to account for the desorption rate constant of adsorbates on the Pt surface.[37]

(39) Kip, B. J.; Duivenvoorden, F. B. M.; Koningsberger, D. C.; Prins, R. *J. Catal.* **1987**, *26*, 105.

(40) Davis, S. M.; Somorjai, G. A. In *The Chemical Physics of Solid Surfaces and Heterogeneous Catalysis*; King, D. A., Woodruff, D. P., Eds.; Elsevier: Amsterdam, 1984; Vol. 4, Chapter 7.

Thus, on the basis of its performance for methylcyclohexane dehydrogenation, the catalyst prepared from $[Re_2Pt(CO)_{12}]$ is regarded as a prototype supported bimetallic cluster catalyst with a maximized Pt dispersion and a maximized resistance to deactivation. Furthermore, the EXAFS data demonstrate that the supported bimetallic clusters have such simple structures that they can be regarded as nearly molecular in character, being modeled as Re_4Pt_2. Like commercial naphtha-reforming catalysts, the catalyst derived from $[Re_2Pt(CO)_{12}]$ consists of an oxophilic metal and a noble metal, with the oxophilic metal contributing to the stability of the noble metal.

Experimental Methods

Catalyst Preparation. Catalysts were prepared by adsorption of $[Re_2Pt(CO)_{12}]$ on γ-Al_2O_3 followed by thermal treatment to remove the carbonyl ligands. Salt-derived γ-Al_2O_3-supported Pt (0.36 wt % Pt) and Re−Pt catalysts (0.32 wt % Pt and 0.59 wt % Re) were prepared from aqueous solutions of the precursors $[Pt(NH_3)_4](NO_3)_2$ and NH_4ReO_4 by the incipient wetness technique. The catalyst preparations are described in detail elsewhere.[2]

Catalyst Testing. The catalysts were tested in a fixed-bed flow reactor with an inside diameter of 1.3 cm. Conversion of methylcyclohexane was measured as a function of time on stream with reactants flowing at a constant rate. Methylcyclohexane (Baker, 99%) was degassed, dried with activated 4A zeolite, and stored under dry N_2 before use. It was introduced into the reactant stream at a constant flow rate with a syringe pump. The flowing feed liquid was vaporized and mixed with a flowing preheated mixture of H_2 (Matheson, 99.999%) and He (Matheson, 99.999%). Each of these feed gases was purified by flow through traps containing particles of Cu and activated 4A zeolite to remove traces of O_2 and moisture, respectively. The catalyst powder (50 mg) was mixed with inert particles (Fisher "RR" Alundum, 90 mesh) in the volume ratio of 1 to 10 to minimize bypassing in the reactor.

In the catalysis experiments, the temperature was 400 °C, the pressure atmospheric, and the weight hourly space velocity (WHSV) of methylcyclohexane 9.3 g of methylcyclohexane/(g of catalyst·h). The total gas flow rate was 45 mL (NTP)/min, with a methylcyclohexane/H_2/He volumetric ratio of 1/11/10.

The product vapors were analyzed with an on-line gas chromatograph equipped with flame ionization detectors. Aliphatic hydrocarbons (C_1−C_6) were separated at 65 °C in a 4.6-m × 3.2-mm column packed with 23% SP-1700/Chromosorb P AW. Benzene, methylcyclohexane, and toluene were separated in a 3.1-m × 3.2-mm column packed with 10% TCEP/Chromosorb P AW in series with a 1.5-m × 3.2-mm column packed with 5% Apiezon L on Chromosorb W AW.

In a blank test performed with the reactor packed with inert alundum particles pretreated with flowing H_2 at 500 °C for 4 h, no conversion of methylcyclohexane and H_2 was observed. Catalysts prepared by adsorption of $[Re_2Pt(CO)_{12}]$ (0.33 wt % Pt, 0.59 wt % Re) on γ-Al_2O_3 were loaded into the tubular reactor in a N_2-filled drybox and brought on stream without air exposure. They were treated in flowing H_2 at 400 °C for 4 h [flow rate = 100 mL (NTP)/min] with a heating rate of 5 °C/min. Salt-derived catalysts were dried at 120 °C for 1 h in flowing He followed by heating in flowing H_2 from 120 to 500 °C [flow rate 100 mL (NTP)/min] with a heating rate of 10 °C/min. The reduction was completed by treatment of the sample in flowing H_2 at 500 °C for 4 h. Another γ-Al_2O_3-supported Pt catalyst prepared from a salt precursor was dried at 500 °C for 1 h in flowing He followed by introduction of flowing H_2 at 500 °C; this temperature was held for 4 h to give a different Pt dispersion from that of the similarly prepared sample. After reduction of the catalyst, the reactor was cooled in flowing H_2 to 400 °C before the flow of reactants was started.

Hydrogen Chemisorption. Hydrogen chemisorption experiments were carried out with a Micromeritics Chemisorb 2800 instrument to determine H/Pt ratios as a measure of the fraction of the Pt exposed in the supported Pt catalysts. Such experiments were not attempted for the Re−Pt catalysts because of the uncertainty in the H/metal stoichiometry that would be needed to estimate the fraction of metal exposed.

EXAFS Data Collection. EXAFS data were collected at Station C-2 of the Cornell High Energy Synchrotron Source (20−40 mA, 5 GeV), which was equipped with a detunable channel-cut Si(111) monochromator. Data were also collected at beamline X-11A of the National Synchrotron Light Source at Brookhaven National Laboratory (2.5 GeV, 60−145 mA) with a Si(111) monochromator, and at the wiggler station 9.2 at the Synchrotron Radiation Source of the Daresbury Laboratory, Daresbury, UK (1.9 GeV, 100−200 mA) with a Si(220) monochromator. All experiments were performed in transmission with optimized ion chambers. Each monochromator was detuned at 50% to minimize contamination arising from higher harmonics. The internal consistency of the data collected at the different stations was always checked with EXAFS data obtained with a standard 3.5-mm Pt foil. Differences in amplitude were no more than 10% from one data set to another. Precautions were taken to optimize all the EXAFS spectrometers and data collecting procedures to maximize the signal-to-noise ratio. Measurements of the samples were done at the Re L_{III} (10534 eV) and Pt L_{III} (11564 eV) edges.

Each sample was pressed to give a self-supporting wafer in a sample holder, with the amount calculated to yield optimal absorption measurements ($\mu x = 2.5$) at the Re L_{III} and Pt L_{III} edges. The sample holder was mounted in a heatable and evacuable EXAFS cell equipped with thin Be windows. Sample treatments at high temperature and transmission measurements at liquid nitrogen temperature were performed with the sample in the same cell, protected from exposure to air.

The samples were treated in H_2 (99.999% purity, 100 mL/min, with a heating rate of 5 °C/min) at 400 °C for 4 h and cooled in flowing H_2 to room temperature. Data were collected with samples under static H_2 at approximately liquid nitrogen temperature.

EXAFS data were also obtained at liquid nitrogen temperature for a series of compounds used as references in data analysis. Re powder (average particle size, 3−4 mm, 99.99% purity, Goodfellows) was mixed with γ-Al_2O_3 and pressed into a self-supporting wafer. The sample in the EXAFS cell was reduced in H_2 at 400 °C for 1 h and cooled in flowing H_2. The other reference compounds were Pt foil (Goodfellows, 3.5 mm), $Na_2Pt(OH)_6$, NH_4ReO_4 (Alfa), K_2ReCl_6 (Alfa), and Na_2PtCl_6 (Strem). They were used as supplied, and the powder samples were mixed with γ-Al_2O_3 to achieve an optimal absorption of $\mu x = 2.5$ with $\Delta\mu x = 1$.

EXAFS Data Analysis

Data Reduction and Analysis Methods. Standard procedures were used to extract the EXAFS data from the measured absorption spectra. Normalization was done by dividing the absorption intensities by the height of the absorption edge and subtracting the background by using cubic spline routines.[24]

The spectra were analyzed by using an improved version of the Utrecht/Eindhoven EXAFS data analysis software (XDAP), including statistical analysis. The statistical analysis is based upon the methods described elsewhere.[41] The parameters extracted from the measurements are the previously defined N, R, $\Delta\sigma^2$, and ΔE_0 (each of the latter with respect to the appropriate reference compound) for the various coordination shells. In this investigation, a k^0 weighting was used for the primary fit. The program allowed simultaneous monitoring of the k^n-weighted fits in k space and in r space as well as the sum of the squares of the residuals between the fit and the data for the k^n-weighted function and for both the magnitude and the imaginary parts of the Fourier transform.

The difference file technique was applied together with phase-corrected Fourier transforms to identify the different contributions in the EXAFS data.[5] Control of the difference files with application of both k^1 and k^3 weighting is required for good fitting as the dependence of k on the backscattering amplitude of low-Z elements (such as O) is different from that on the backscattering amplitude of high-Z elements (such as Re and Pt); the backscattering amplitude of a low-Z element becomes very small at $k < 7$ Å^{-1}, whereas that of a high-Z scatterer is still significant at higher values of k.[5] Optimization of both the k^1- and k^3-weighted fits also results in a better decoupling of the EXAFS

(41) Vaarkamp, M. Ph.D. Dissertation, Eindhoven University of Technology, The Netherlands, 1992, Chapter 2.

Table 5. Crystallographic Data and Fourier Transform Ranges Used for the Fabrication of the EXAFS References

compd	A−B[a]	R (Å)[b]	N[c]	ref	n[d]	Fourier range Δk (Å^{-1})	Fourier filter ΔR (Å)
Re powder	Re−Re	2.74	12	47	3	2.9−16.4	1.7−3.4
Pt foil	Pt−Pt	2.77	12	47	3	2.0−19.8	1.9−3.0
$NH_4[ReO_4]$	Re−O	1.74	4	48	3	2.9−13.8	0.8−2.5
$Na_2[Pt(OH)_6]$	Pt−O	2.05	6	49	3	2.8−15.3	0.8−2.5
$K_2[ReCl_6]$	Re−Cl	2.36	6	50	3	2.4−13.6	1.1−2.7
$Na_2[PtCl_6]$	Pt−Cl	2.32	6	51	3	2.2−13.7	1.1−2.7

[a] A−B: absorber−backscatterer pair. [b] R: coordination distance. [c] N: coordination number. [d] n: exponent of the weighting factor of Fourier transformation.

parameters (N and $\Delta\sigma^2$; R and ΔE_0).[5] In some cases the EXAFS coordination numbers N_E obtained in the data analysis had to be corrected for the difference in distance between the absorber−backscatterer pair of the reference shell and that of the shell to be analyzed. This correction is required because the factor $\exp(-2R/\lambda)$ in the EXAFS formula is not always negligible.[5] The correct coordination number N is therefore $N_E/\exp\{-2(R - R_{ref})/\lambda\}$ with λ taken to be equal to 6 Å, which is a good approximation for values of $k > 3$ Å^{-1}.[5]

Reference Data. EXAFS data obtained for reference compounds were analyzed first to obtain in pure form the contribution of each absorber-backscatterer pair. Table 5 includes a summary of the Fourier transform range (k_{min} and k_{max}) and the crystallographic data characterizing the first coordination shell of each reference compound. The valid range in k space for use of the reference compounds in modeling each absorber−backscatterer pair is between ($k_{min} + 0.5$) Å^{-1} and ($k_{max} - 0.5$) Å^{-1}. This practice minimizes the truncation errors caused by the Fourier transformation of the raw EXAFS function.[42]

Re−Pt and Pt−Re Absorber−Backscatterer Pair. The absence of a suitable reference compound for the Re−Pt and Pt−Re pairs leads to difficulty in analyzing the bimetallic contribution in the EXAFS data. Although $[Re_2Pt(CO)_{12}]$ would at first appear to be an appropriate reference for the Re−Pt pairs, the overlap of the Re−Pt peak with the Re carbonyl contribution, Re···O*, in the Fourier transform of the Re L_{III} edge hinders the correct identification and extraction of the RePt contribution by inverse transformation (the Re−Pt distance is 2.83 Å, and the Re···O* distance is 3.12 Å).[43] Moreover, if one attempts to derive the Re−Pt contribution by first subtracting the Re carbonyl contribution from the experimental EXAFS function, the presence of only one Pt neighbor about each Re atom may lead to a large uncertainty in deriving the normalized amplitude function. The same problem arises in obtaining a Pt−Re interaction from data for $[Re_2Pt(CO)_{12}]$. Therefore, the Re−Pt and Pt−Re phase shift functions and backscattering amplitudes were composed by using other reference compounds.

The normalized backscattering amplitude [$F^*(k)$] (defined by Vaarkamp *et al.*[44]) has been found to be a function of the backscattering atom.[45] The function $F^*(k)$ is generally the same for the absorber−backscatterer pairs A−B and A′−B, where A and A′ are different absorbers.[45] Therefore, $F^*(k)$ for the Re−Re pair can be used for the Pt−Re pair, and vice versa for the Pt−Pt and Re−Pt pairs.

$$F^*_{Pt-Re}(k) = F^*_{Re-Re}(k) \quad (5)$$

$$F^*_{Re-Pt}(k) = F^*_{Pt-Pt}(k) \quad (6)$$

The property of the additivity and the transferability of the phase shift function[45] is used to compose the Re−Pt and Pt−Re contributions. According to theory,[45] the phase shift function of the absorber (A)−backscatterer (B) pair X−Y consists of a linear combination of $\varphi_A(X)$, due to the absorbing atom X, and $\varphi_B(Y)$, due to the backscattering atom B, in the L_{III} absorption edge.

$$\varphi(X-Y) = 2\varphi_A(X) + \varphi_B(Y) \quad (7)$$

This implies that Re−Pt and Pt−Re phase shift functions can be determined by using a combination of phase shift functions derived from other reference compounds such as Pt foil, Re powder, K_2ReCl_6, and Na_2PtCl_6. Sinfelt *et al.*[46] used this approach to analyze data for a supported Ru−Cu catalyst with theoretical phase shift functions. The Re−Pt and Pt−Re phase shift functions reported here are composed from the following combination of experimental phase shift functions:

$$\varphi(Pt-Re) = \varphi(Pt-Cl) + \varphi(Re-Re) - \varphi(Re-Cl) \quad (8)$$

$$\varphi(Re-Pt) = \varphi(Re-Cl) + \varphi(Pt-Pt) - \varphi(Pt-Cl) \quad (9)$$

As a result, the relative energy (inner potential correction) (ΔE_0) obtained in the EXAFS data analysis for the Re−Pt and Pt−Re pairs is only an adjustable parameter and does not reflect any physical significance in the relative difference of the chemical environment between the sample and the reference.

Distinguishing Re and Pt Backscatterers in EXAFS Data Analysis. Re and Pt are only five positions apart from each other in the periodic table, and it has normally been assumed that it is not possible to distinguish between neighboring Re and Pt atoms in the

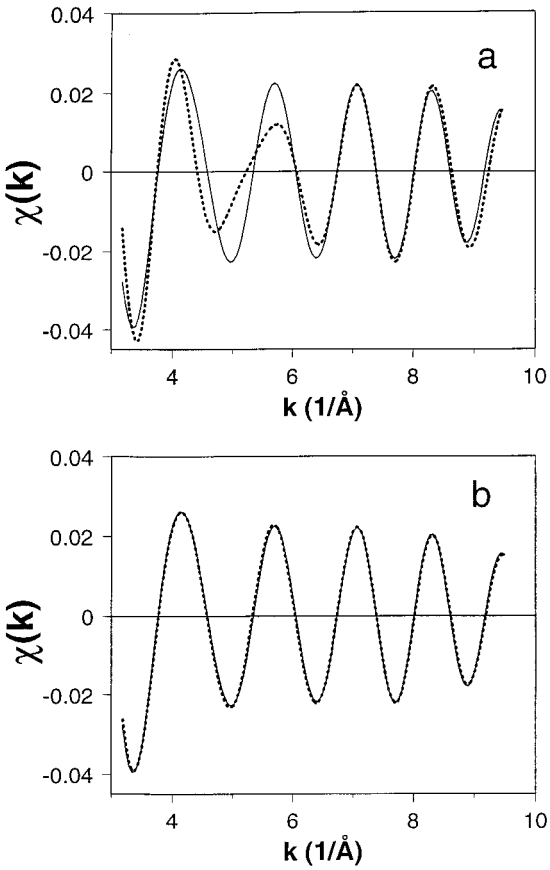

Figure 9. (a) Model Pt−Re EXAFS function (solid line) (calculated with Pt−Re reference with input parameters given in Table 6) and fit (with Pt−Pt as reference, fit of results given in Table 5). (b) Model Pt−Re EXAFS (see part a) (solid line) and fit (with Re−Re as reference, fit of results given in Table 6).

(42) Vaarkamp, M.; Dring, I.; Oldman, R. J.; Stern, E. A.; Koningsberger, D. C. *Phys. Rev. B Condens. Matter* **1994**, *50*, 7872.
(43) Urbancic, M. A.; Wilson, S. R.; Shapley, J. R. *Inorg. Chem.* **1984**, *23*, 2954.
(44) Vaarkamp, M.; Linders, J. C.; Koningsberger, D. C. *Physica B* **1995**, *208* and *209*, 159.
(45) Teo, B. K.; Lee, P. A. *J. Am. Chem. Soc.* **1979**, *101*, 2815.
(46) Sinfelt, J. H.; Via, G. H.; Lytle, F. W. *J. Chem. Phys.* **1980**, *72*, 4832.
(47) Kittel, C. *Introduction to Solid State Physics*, 6th ed., Wiley: New York, 1986; p 24.
(48) Brown, R. J. C.; Segel, S. L.; Dolling, G. *Acta Crystallogr.* **1980**, *B36*, 2195.
(49) Troemel, M.; Lupprich, E. *Z. Anorg. Allg. Chem.* **1975**, *414*, 160.
(50) Grundy, H. D.; Brown, I. D. *Can. J. Chem.* **1970**, *48*, 1151.
(51) Williams, R. J.; Dillin, D. R.; Milligan, W. O. *Acta Crystallogr.* **1973**, *B29*, 1369.

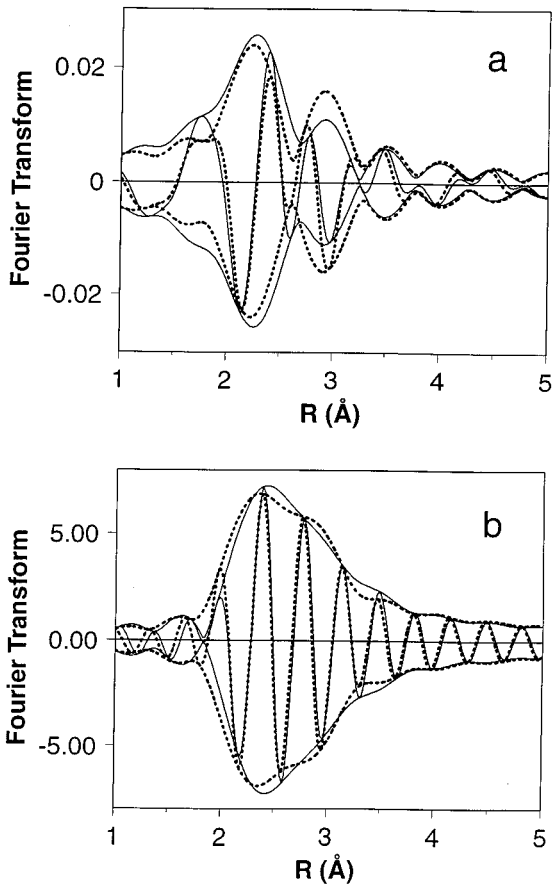

Figure 10. Fourier transform ($\Delta k = 3.5-9.2$ Å^{-1}) of data given in Figure 9a: (a) k^0 weighting and (b) k^3 weighting.

EXAFS data analysis. To investigate this issue, a model Pt−Re EXAFS function was calculated by using the Pt−Re reference function described above. As input parameters for the calculation, the following were used: N (coordination number) = 12; R (coordination distance) = 2.77 Å; $\Delta\sigma^2$ (disorder term) = 0; and ΔE_0 (inner potential correction) = 0. The model function is displayed in Figure 9a (solid line). Fitting this model function with a Pt−Pt reference function by using a k^0-weighted fit in k space (Figure 9a, dotted line) resulted in the coordination parameters given in Table 5. The variance of the fit is only 12.4, and it can be seen in Figure 9a that the fit (using a Pt−Pt reference) at low values of k strongly deviates (both in phase and amplitude) for $4 < k < 6$ Å from the model EXAFS function (calculated with a Pt−Re reference). Thus it can be concluded that $\varphi_B(\text{Pt}) \neq \varphi_B(\text{Re})$ and $F^*_{\text{Pt-Re}} \neq F^*_{\text{Pt-Pt}}$.

Table 6. EXAFS Model Study of Transferability of Pt−Pt, Re−Re, Pt−Re, and Re−Pt Phase Shifts and Backscattering Amplitudes

coordination Pt−Re	ref	N	$10^3\,\Delta\sigma^2$ (Å^2)	R (Å)	ΔE_0 (eV)	variance
model	Pt−Re	12	0	2.77	0	
fit	Pt−Pt	12.4	−1.8	2.72	−0.8	12.4
fit	Re−Re	12.6	0.3	2.74	2.3	0.18

Analyzing the Pt−Re model function with a Re−Re reference leads to the results presented in Table 6. Figure 9b shows a good agreement between the Pt−Re model function (calculated with the Pt−Re reference) (Figure 9b, solid line) and the fit (using a Re−Re reference) (Figure 9b, dotted line). The variance of the fit was found to be 0.18, from which it can be concluded that, in principle, a Re−Re reference can be used to analyze Pt−Re data. It can also be concluded from these results that the Pt absorber phase φ_A(Pt) and the Re absorber phase φ_A(Re) are not detectably different from each other, since the high quality of the fit shows that φ(Pt−Re) and φ(Re−Re) are essentially the same. On the basis of these results, it is also obvious that the backscattering amplitude $F^*_{\text{Pt-Re}}$ is indistinguishable from $F^*_{\text{Re-Re}}$.

In earlier work, k^3 weighting has normally been used in the data analysis. Figure 10a displays a k^0-weighted Fourier transform of the EXAFS data presented in Figure 9a. The differences between the solid line (calculated with a Pt−Re reference) and the dotted line (the result of fitting with a Pt−Pt reference) are clear. In contrast, with the k^3-weighted Fourier transform (Figure 10b) the differences between the dotted line and the solid line are hardly visible. Figure 10 makes clear that a k^3 weighting almost completely minimizes the differences between a Pt and Re backscatterer.

One of the most important conclusions from this model study is that a Pt and a Re neighboring atom can be distinguished. This can only be done if a k^0 weighting is used in the EXAFS data analysis. Moreover, a Pt−Pt (or Re−Re) reference cannot be used to analyze a Pt−Re (or Re−Pt) reference.

Acknowledgment. We thank E. E. Carroll of E. I. du Pont de Nemours and Company for performing the hydrogen chemisorption experiments. This research was supported by the National Science Foundation (Grant CTS-9315340, among others). The international collaboration was supported by a NATO travel grant.

Supporting Information Available: Details of the performance of alumina-supported cluster-derived Re−Pt catalyst (23 pages). See any current masthead for ordering and Internet access instructions.

JA962816Z